Quasi-static Test of Pavilion-Type Timber Frame with Forked Column under Different Axial Compression Ratios

Zuoshuai Sun, Liangjiu Jia*

Dept. of Disaster Mitigation for Structures, College of Civil Engineering, Tongji University, Shanghai 200092, China

Email:Zuoshuai Sun: 2010289@tongji.edu.cn;
Liangjiu Jia: lj_jia@tongji.edu.cn

Abstract. Traditional Chinese pavilion-type timber structure, with more than 2000 years history, is a highly nonlinear structural system with sophisticated seismic mitigation and isolation mechanisms. To investigate seismic deformation process and hysteresis response of the pavilion-type timber frame with forked column, quasi-static test was carried out on a 1/3.4 scaled model of a single-story timber frame. It is found that rotation of mortise-tenon joints, forked column limb bending deformation, Zhutou-Fang bending deformation and other deformation of pavilion-type timber frame with forked column under different axial compression ratios occurred. The larger the axial compression ratios are, the larger the deformation of the forked column limb and the Zhutou-Fang is, as well the bottom boundary condition of the forked column limb is changed from hinge to fixed with the axial compression ratios increasing. Besides, when the inter-story drift is 1/30, Ludou of the invisible paving layer of the timber frame appears to compression cracks.

Keywords: pavilion-type timber frame; forked column; quasi-static test; hysteresis response

1 INTRODUCTION

Ancient Chinese traditional pavilion-type timber structures contain a wealth of architectural wisdom and are a valuable cultural heritage. Representative ones include the Yingxian Pagoda and the Guanyin Pavilion of Jixian County, among which the Yingxian Pagoda is the most famous and studied. The Yingxian Pagoda, built in 1056 AD, is the tallest pagoda in the world and consists of five visible layers and four invisible layers, and each of these layers consists of column base layer, column frame layer and paving layer. The nonlinear response of each structural layer under the effect of earthquake shows that the Yingxian Pagoda is a highly nonlinear structural system, which contains a wealth of damping and isolation mechanism [1], and its seismic mechanism is complex and has not been fully revealed.

B. Yuan et al. (eds.), *Proceedings of the 2024 8th International Conference on Civil Architecture and Structural Engineering (ICCASE 2024)*, Atlantis Highlights in Engineering 33,
https://doi.org/10.2991/978-94-6463-449-5_45

Japanese scholars have been studying the five-storied pagoda, which is also belong to the pavilion-type structure, for a century, Tanahashi [2] pointed out that the self-centering capacity of timber frame mainly relies on gravity to reset itself. Corresponding to the research of Yingxian Pagoda, the relevant research showed its good seismic performance and it was found that there is a switch between the fixed and rocking state. However, the pavilion-type timber frame is highly nonlinear, and the deformation mechanism is more complex than that of a single rocking structure [3]. Most of the current studies focus on the seismic performance and deformation mechanism of the independent timber frame members, including the rotation performance of mortise-tenon joints [4] and Dougong [5], the seismic performance of column frame layer and paving layer [6-8]. There are fewer studies on the combined timber frame based on the previous studies. Therefore, based on the visible layer and invisible layer of Yingxian Pagoda, the quasi-static test of a 1/3.4 scaled pavilion-type timber frame with forked column was carried out, which is no longer a confined member study. Detailed deformation analysis of the forked column limbs and Zhutou-Fang was carried out to clarify the hysteresis performance of the forked column limbs and the coordinated deformation process with the combined timber frame. At the same time, the seismic performance of different stories of Yingxian Pagoda still has differences, which needs further research. The deformation of forked column limbs in the combined timber frame with different axial compression ratios was analyzed in the paper, and the results show that the forked column limbs mainly undergo bending deformation with two different boundary conditions caused by different axial compression ratios. In addition, the deformation of Ludous and Zhutou-Fangs were also analyzed to fully reveal the deformation process of critical members in the combined timber with different axial compression ratios.

2 OVERVIEW OF THE TEST

In this study, the timber frame of outside groove span of Yingxian Pagoda was selected as the test object. According to the principle of materials financial separation with 17mm in the construction of Yingxian Pagoda based on Yingzaofashi, considering the size limitations of the test loading frame, the specimen scaled ratio is a 1:3.4. The specimen structure, as shown in Fig. 1, mainly including the column frame layer of the visible layer and the paving layer of the invisible layer, the two parts are connected through the forked columns. The upper part of the specimen includes columns and Lane, which are connected by mortise-tenon joints, and the bottom part of the specimen consists of Dougongs and Fangs, as shown in Fig. 1, which are connected by Sandou and wooden pins.

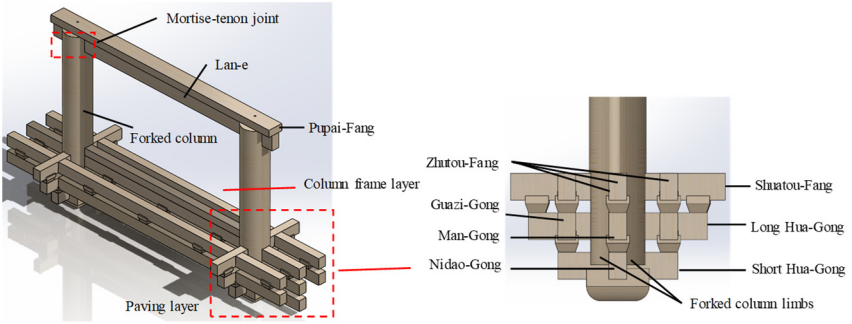

Fig. 1. Structure of specimen

The test setup is shown in Fig. 2 (a), the bottom of the specimen is connected with the wood plate to model the connection between the Ludou of invisible layer and the PuPai-Fang; The wood pads are arranged between the connection plate of the loading device and the Lan-e to realize the free boundaries of the Lan-e and the Pupai-Fang to ensure the consistency of the test with the boundaries of the prototype structure. The arrangement of displacement transducer and strain gauge is shown in Fig. 2 (b), the forked column displacement transducers are arranged at the outer column limb to measure the horizontal displacement; the displacement transducers are arranged at the two sides, and the displacement transducers of the Zhutou-Fang is arranged at the two ends of the top paving layer to collect the vertical displacement. According to the principle that the stress ratio with 1:1 to determine the top loads are 12.7 kN, 56.5 kN, and 76.7 kN, corresponding to the second, third, and fifth story of Yingxian Pagoda, respectively. The three test conditions are TF-006, TF-023, and TF-034, as shown in Tab. 1. In addition, the material used for the specimen is larch which is consistent with the prototype structure, and the test results summary is shown in Tab.2.

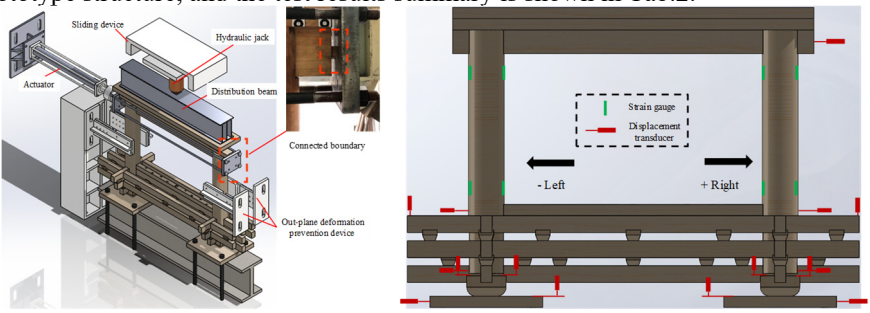

(a) (b)

Fig. 2. (a) Test setup (b) Test instrumentation and measurement

Table 1. Test conditions

	TF-006	TF-023	TF-034
N(*kN*)	12.7	56.5	76.7
Axial compression ratio	0.006	0.023	0.034

Table 2. Material test results summary

Compression elastic modulus (MPa)			Compression strength (MPa)				Moisture content (%)	Density (g/cm^3)
parallel to grain	perpendicular to grain		parallel to grain	perpendicular to grain				
	Radial	Tangential		Radial	Tangential	Oblique		
10192.86	1110.98	498.17	47.20	6.28	12.12	2.92	11.77	0.46

Based on the cyclic protocol in the standard ISO-16670 (ISO 2003) and protocol for testing timber frame structures, a displacement-controlled cyclic loading protocol, as illustrated in Fig. 3, is determined to be adopted. The loading process was carried out starting from an inter-story drift of 1/2400 in order to first check the loading equipment and the measuring system. Thereafter loading was performed cyclically according to 0.075Δ, 0.1Δ, 0.2Δ, 0.3Δ, 0.5Δ, 0.6Δ, Δ. According to GB 50165-92 1992, in the seismic deformation calculation, the limit of timber frame inter-story drift is Δ = 1/30.

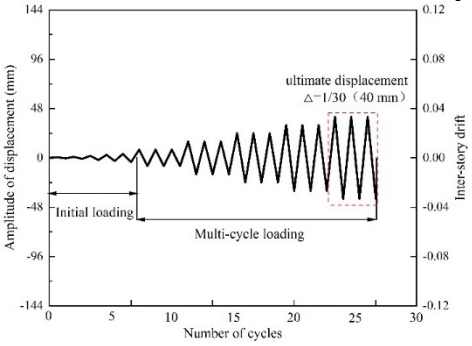

Fig. 3. Loading protocol

3 TEST PHENOMENON AND HYSTERESIS CURVES

The hysteresis curves of TF-006, TF-023 and TF-034 and the corresponding test phenomena are shown in Fig. 4. Under the three working conditions, the rotation of mortise-tenon joints and the rotation of forked column limbs mainly occurred in the initial loading stage, and as the displacement loading level increased to 4mm, the rotation of the Shuatou-Fang and the phenomenon of Difu opening and the compression deformation between the column head and Pupai-Fang occurred. As the displacement loading level increases to 8mm, three Zhutou-Fangs from top to bottom successively

bending and then common bending. However, the bottom boundary of the forked column limb of TF-006 is hinge during the loading process, while that of TF-023 and TF-034 are fixed. Which leads to the difference in the stiffness of the timber frame under the action of different axial compression ratios, and with the increase of axial compression ratio, the gaps among the members are completely closed. The initial stiffness of TF-023 increased by 64.6% relative to that of TF-006, the initial stiffness of TF-034 increased by 118.5% compared to that of TF-006, and the initial stiffness of TF-034 increased by 32.7% compared to that of TF2. The bearing capacity of TF-023 increased by 127.4% compared to that of TF-006, the bearing capacity of TF-034 increased by 184.2% compared to that of TF-006, and the bearing capacity of TF-034 increased by 25% compared to that of TF023. As shown in Fig. 4, compression-bearing cracks appeared in the bottom Ludou when TF-034 was loaded to inter-story drift of 1/30, while no damage was seen in TF-006 and TF-023 during the loading process.

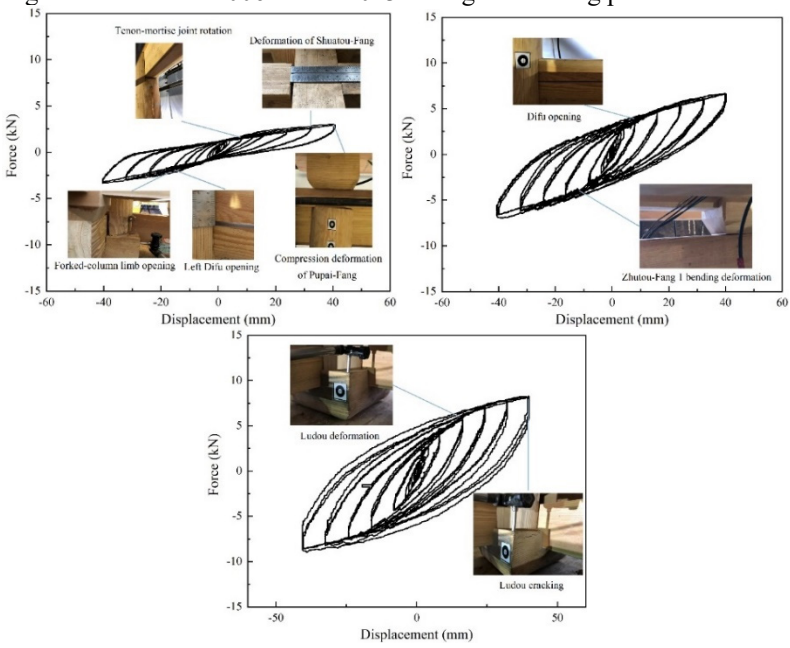

Fig. 4. Hysteresis curves and test phenomenon

4 HYSTERESIS CHARACTERISTICS ANALYSIS

Analyze the deformation of the visible layer components, including the deformation of the column base and that of the forked column limbs .Under the action of different axial compression ratios, the horizontal displacement of the column base with loading level as shown in Fig. 5, the results show that, with the increase of axial compression ratio, the displacement of the column base increases with the familiar linear trend, indicating that the columns are in the elastic deformation state, and the column frame layer occurs in the mortise-tenon joint rotation and the forked column limb bending deformation.

The deformation of the forked column limbs is then analysed, as shown in Fig. 6. Compared with TF-023 and TF034 with large axial compression ratio, the displacement curves of the fork column limbs of TF-006 with small axial compression ratio are obviously different, and the deformation of the forked column limbs under the same horizontal displacement loading level is smaller. This is because of the different boundary conditions at the bottom of the fork column limbs. Under the condition of small axial pressure ratio TF-006, the forked column limb is not in contact with the bottom Ludou during the loading process, and there is no restriction, the right forked column limbs when loading in the positive direction and the left forked column limbs when loading in the negative direction are coordinated with the column deformation during the loading process first, and then after the bending deformation, the displacement is 0 when the maximum loading horizontal displacement is applied; Similarly, due to the lack of constraint at the bottom of the fork column limbs, the deformation of the right forked column limbs when loading in the negative direction are always in coordination with the column deformation, but the deformation of the left forked column limbs during positive loading are not harmonized with the deformation of the column, which is due to the existence of a horizontal initial gap between the outer forked column limbs and the Dougongs, which belongs to the defects of the processing and installation. Under the conditions of TF-023 and TF-034 with large axial compression ratio, the bottom of the forked column limbs is always in contact with the Ludou during the loading process, and the displacement shows a linear trend, which is harmonized with the deformation of the column.

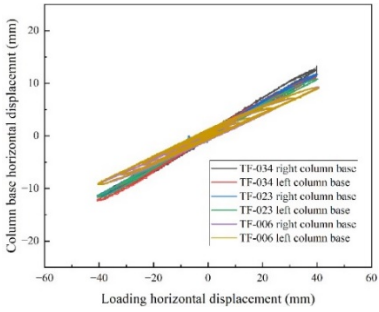

Fig. 5. Column base horizontal displacement of timber frame with different axial compression ratios

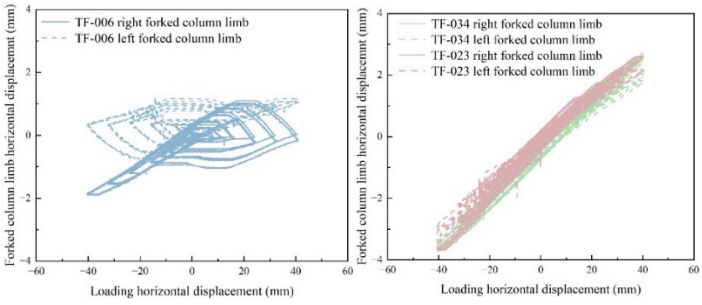

Fig. 6. Deformation of forked column limb

And then analyze the deformation of the invisible layer components, including the deformation of the Zhutou-Fang and that of the bottom Ludous. The vertical displacement of Zhutou-Fang under horizontal displacement loading is shown in Fig. 7. The deformation trend of Zhutou-Fang under the three conditions is the same, indicating that the third Zhutou-Fang has undergone bending deformation. The larger the axial compression ratio is, the larger the vertical deformation is after the initial axial force is applied, indicating that the bottom of the column is completely closed with Shuatou-Fang and the third Zhutou-Fang, and the vertical deformation of the Zhutou-Fang increases with the increase of the axial compression ratio. Furthermore, the displacement of the bottom Ludous under horizontal displacement loading is shown in Fig. 8, with the increase of axial compression ratio, the compressive deformation of the bottom Ludous increases. Due to the forked column limbs of TF-006 are not in contact with the bottom of Ludous, the vertical displacement of the Ludous is small, and the vertical force that produces deformation is transmitted from the short Hua-Gong to the Ludous.

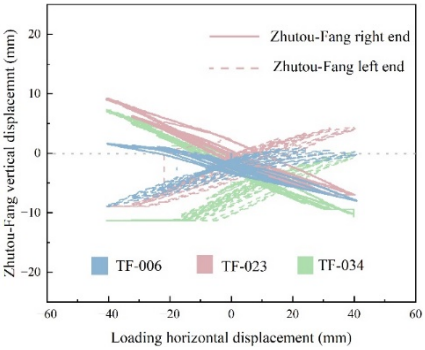

Fig. 7. Zhutou-Fang vertical displacement

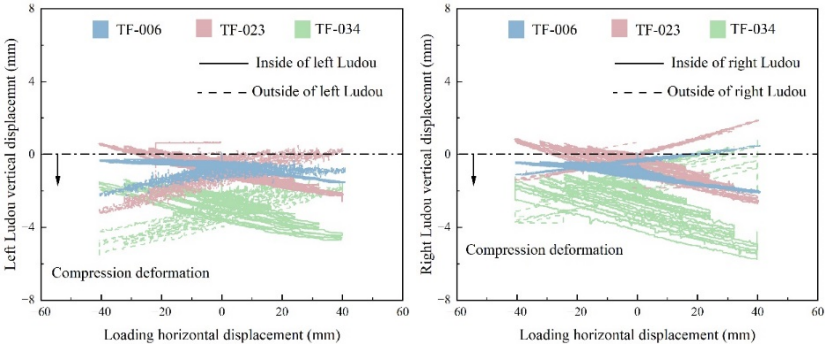

Fig. 8. Ludou vertical displacement

5 CONCLUSION

(1) Rotation of the mortise-tenon joints, opening and closing of the Difu, compressive deformation between the column head and the Pupai-Fang, compressive deformation

of the Ludous and bending deformation of the Zhutou-Fangs of TF-006, TF-023 and TF-034 were occurred during the lateral displacement loading process.

(2) Hysteresis curves of TF-006, TF-023 and TF-034 under horizontal loading are full, indicating the timber frame with forked column limbs have the good energy dissipation capacity. When loaded to the inter-story drift of 1/30, the horizontal load of TF-023 is 127.4% larger than that of TF-006, the horizontal load of TF-034 is 184.2% larger than that of TF-006, and the horizontal load of TF-034 is 25% larger than that of TF-023.

(3) Whether the forked column limb is in contact with the Loudous of invisible layer or not under vertical load is the criterion for judging the deformation state of the timber frame, the initial stiffness of TF-023 is 64.6% larger than that of TF-006, the initial stiffness of TF-034 is 118.5% larger than that of TF-006, and the initial stiffness of TF-034 is 32.7% larger than that of TF-023.

Although in this paper, the proposed quasi-static test of the timber frame with forked column was carried out and hysteresis analysis and deformation process analysis were completed, the related deformation mechanism has not been fully elucidated, and the theoretical model of this timber frame needs to be proposed, while the dynamic characteristics and seismic performance of the multi-story pavilion-type timber frame are still a future research direction.

REFERENCES

1. Ishiyama Y. (1984) Motions of rigid bodies and criteria for overturning by earthquake excitations. Earthquake Engineering and Structural Dynamics. 10(5): 635–650. https://doi.org/10.1002/eqe.4290100502.
2. Tanahashi H, Shimizu H, Suzuki YF. (2010) Seismic and Wind Performance of Five-Storied Pagoda of Timber Heritage Structure. Advance in Material Research. 133–134:79–95. https://doi.org/10.4028/wwwscientific.net/AMR.133-134.79.
3. Sun Z, Xiang P, Jia L. (2022) Seismic response and kinematic mechanisms of single-story pavilion-type timber frame based on shaking table test. Structures, 2022(45): 1701-1716. https://doi.org/10.1016/j.istruc.2022.10.016.
4. Xie Q, Wang L, Zheng P. (2018) Rotational behavior of degraded traditional mortise-tenon joints: Experimental tests and hysteretic model. International Journal of Architectural Heritage, 12(1): 125–136. https://doi.org/10.1080/15583058.2017.1390629.
5. Li X, Zhao J, Ma G. (2015) Experimental study on the seismic performance of a double-span traditional timber frame. Engineering Structures, 98: 141–150. https://doi.org/10.1016/j.engstruct.2015.04.031.
6. Meng X, Li T, Yang Q. (2019) Experimental study on the seismic mechanism of a full-scale traditional Chinese timber structure. Engineering Structures, 180: 484–493. https://doi.org/10.1016/j.engstruct.2018.11.055.
7. Chen J, Chen Y, Shi X. (2018) Hysteresis behavior of traditional timber structures by full-scale tests. Advances in Structural Engineering, 21(2): 287–299. https://doi.org/10.1177/1369433217717117.
8. Xue J, Wu Z, Zhang F. (2015) Seismic damage evaluation model of Chinese ancient timber buildings. Advances in Structural Engineering, 18(10): 1671–1683. https://doi.org/10.1260/1369-4332.18.10.1671.